A new ternary compound with the BGa8Ir4 structure type in the Al-Au-Ir system

Joris Kadok, Marie-Cécile de Weerd, Pascal Boulet, Vincent Fournée, Julian Ledieu

STRUCTURAL SCIENCE
CRYSTAL ENGINEERING
MATERIALS

ISSN 2052-5206

A new ternary compound with the BGa_8Ir_4 structure type in the Al–Au–Ir system

Joris Kadok, Marie-Cécile de Weerd, Pascal Boulet, Vincent Fournée and Julian Ledieu*

Institut Jean Lamour (UMR7198 CNRS, Université de Lorraine), Campus ARTEM 2 allée André Guinier, 54011 Nancy Cedex, France. *Correspondence e-mail: julian.ledieu@univ-lorraine.fr

Received 15 October 2018
Accepted 23 November 2018

Edited by M. de Boissieu, SIMaP, France

Keywords: intermetallic; X-ray diffraction; crystal structure; entropy.

CCDC reference: 1881225

Supporting information: this article has supporting information at journals.iucr.org/b

Following the recent determination of the Al_3AuIr structure, a new ternary phase has been identified in the Al–Au–Ir phase diagram. It has a chemical composition $Al_9(Au;Ir)_4$ with an apparently low gold content. Its crystal structure has been determined with single-crystal X-ray diffraction. The new compound crystallizes in the tetragonal crystal system and has been successfully solved in space group $I4_1/acd$ (Pearson symbol $tI104$) with lattice parameters a = 8.6339 (2) and c = 21.8874 (7) Å. Atomic environments are described as well as similarities with the BGa_8Ir_4 compound.

1. Introduction

The Al–Ir system has several intermetallic compounds in the Al-rich part of the phase diagram: Al_9Ir_2, $Al_{45}Ir_{13}$, $Al_{28}Ir_9$, $Al_{2.75}Ir$ and AlIr (Okamoto, 2009). The crystal structures of the compounds in this system can be of great complexity. Indeed, the $Al_{45}Ir_{13}$ and $Al_{28}Ir_9$ compounds crystallize in their own structure type, both containing 236 atoms in their respective unit cell. The Al–Au system also includes several intermetallic compounds across the whole range of the phase diagram: Al_2Au, AlAu, $AlAu_2$, Al_3Au_8 and $AlAu_4$ (Okamoto, 1991). The crystal structures of these compounds are simpler than those from the Al–Ir system with the exception of the Al_3Au_8 phase which has 132 atoms in the unit cell (In_3Yb_8 structure type).

Unlike the two Al–Ir and Al–Au systems, Au and Ir are not miscible and do not form any intermetallic compound. According to Dubois & Belin-Ferré (2011), structurally complex metallic alloys (CMAs) are likely to be found in ternary systems like Al–Au–Ir in which two transition elements are immiscible. CMAs are of great interest as they exhibit unique properties that differ from those of their main constituents or structurally simpler compounds. Recently, investigation of the Al–Au–Ir system has revealed the existence of the Al_3AuIr compound (Kadok *et al.*, 2015). This compound is of the Ni_2Al_3 structure type and exhibits a split Al atomic position originating from the mixed occupancy of another Au/Ir atomic position. *Ab initio* calculations suggested a Hume–Rothery stabilization mechanism for this Al_3AuIr compound. The present report follows the exploration of the Al–Au–Ir system and introduces the new $Al_9(Au;Ir)_4$ compound. The crystal structure of this new ternary phase has been determined with single-crystal X-ray diffraction and will be presented and discussed.

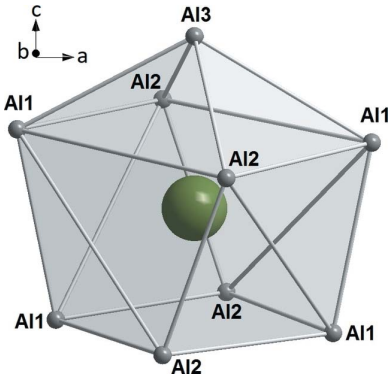

Table 1
Experimental details for $Al_9(Au;Ir)_4$.

Crystal data	
Chemical formula	$Al_{72}Au_{2.5}Ir_{29.5}$
M_r	8104.88
Crystal system, space group	Tetragonal $I4_1/acd$
Temperature (K)	296
a, c (Å)	8.6339 (2), 21.8874 (7)
V (Å^3)	1631.58 (9)
Z	1
Radiation type	Mo $K\alpha$
μ (mm^{-1})	66.45
Crystal size (mm)	0.05 × 0.05 × 0.01
Data collection	
Diffractometer	Bruker APEX-II QUAZAR CCD
Absorption correction	Multi-scan†
T_{min}, T_{max}	0.274, 0.749
No. of measured, independent and observed [$I > 2\sigma(I)$] reflections	44 132, 1629, 1177
R_{int}	0.064
$(\sin\theta/\lambda)_{max}$ (Å^{-1})	0.983
Refinement	
$R[F^2 > 2\sigma(F^2)]$, $wR(F^2)$, S	0.017, 0.043, 1.13
No. of reflections	1629
No. of parameters	35
	$w = 1/[\sigma^2(F_o^2) + (0.0139P)^2 + 16.567P]$ where $P = (F_o^2 + 2F_c^2)/3$
$\Delta\rho_{max}$, $\Delta\rho_{min}$ (e Å^{-3})	4.05, −1.85

† *SADABS* 2014/5 (Krause *et al.*, 2015).

2. Experimental details

A sample weighing 0.3 g with a nominal composition of $Al_{69}Au_3Ir_{28}$ was first prepared by arc melting under 50 kPa of argon from materials of high purity. The sample was inverted and remelted several times to ensure homogeneity. A mass loss of about 2% occurred due to the known evaporation of Al during the synthesis. The resulting ingot was deposited in a capped alumina crucible, sealed in an evacuated quartz tube filled with 70 KPa of an He 90%/H_2 10% gas and annealed at 1173 K for 336 h. Characterization of the phases has been carried out using powder X-ray diffraction (PXRD) on a D8 Advance Bruker diffractometer using Cu $K\alpha_1$ radiation (λ = 1.54056 Å). Single-crystal X-ray diffraction (SC-XRD) data were collected on a Bruker Kappa APEX-II diffractometer equipped with a mirror monochromator and a Mo $K\alpha$ microfocus source (IμS, λ = 0.71073 Å). The *APEX2* program package (Bruker, 2004) was used for the cell refinements and data reductions. The crystal structure was solved using direct methods and refined with the *SHELXL*-2013 program (Sheldrick, 2008). Semi-empirical absorption correction (*SADABS*; Krause *et al.*, 2015) was applied to the data. The sample was also mechanically polished to a maximum grain size of 0.25 µm and micrographs were obtained with scanning electron microscopy (SEM) in a Philips XL30S-FEG. Local chemical compositions were obtained in SEM with energy-dispersive X-ray spectroscopy (EDS) and with wavelength-dispersive X-ray spectroscopy (WDS) on a Jeol 8530-F electron microprobe.

3. Results and discussion

3.1. General observations

The PXRD pattern of the sample after the heat treatment is presented in Fig. 1. This pattern can be partially indexed with diffraction peaks from the two known AlIr and Al_3AuIr compounds. The remaining reflections cannot be attributed to any other known Al–Ir or Al–Au binary compound, hence suggesting the stabilization of a new ternary phase. The presence of three phases could be confirmed with SEM analysis. Fig. 2 shows a SEM micrograph of a section of the sample taken in back-scattered electron (BSE) mode. Two phases in two different shades of grey can be identified on this picture. Black areas are pores in the sample.

From EDS analysis, the light grey and dark grey phases correspond, respectively, to the Al_3AuIr compound and to a ternary Al–Au–Ir composition with a low gold content. As determined by SEM analysis, the latter is the dominant phase

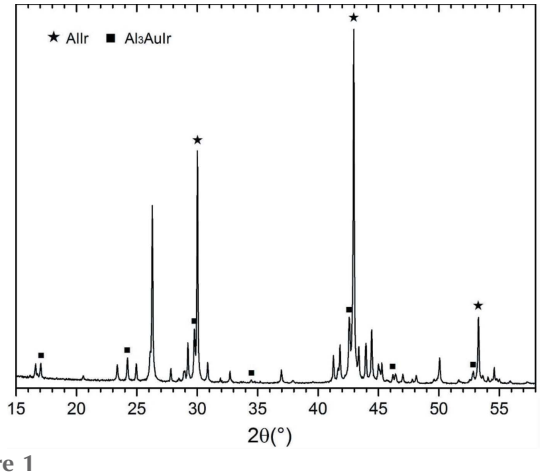

Figure 1
PXRD pattern of the annealed sample obtained with Cu $K\alpha_1$ radiation (λ = 1.54056 Å). Aside from the known AlIr and Al_3AuIr phases, the remaining peaks correspond to the new ternary compound.

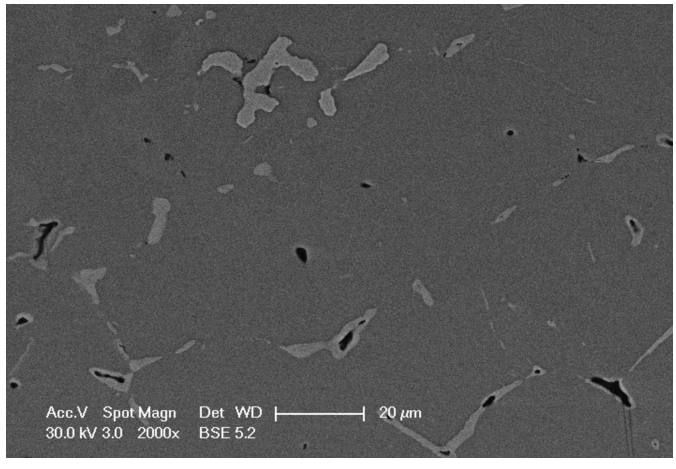

Figure 2
A scanning electron micrograph of the polished sample obtained in BSE mode. The light grey phase corresponds to Al_3AuIr and the dark grey one to the new ternary compound. Black areas are pores.

Table 2
Fractional atomic coordinates and equivalent isotropic displacement parameters for $Al_9(Au;Ir)_4$.

Atom	Site	x	y	z	U_{eq} (Å^2)	Occupancy
Au1/Ir1	16*d*	0	$\frac{1}{4}$	0.01467 (2)	0.00316 (4)	0.08/0.92
Au2/Ir2	16*f*	0.19858 (2)	0.44858 (2)	$\frac{1}{8}$	0.00368 (3)	0.08/0.92
Al1	32*g*	0.04687 (12)	0.03071 (12)	0.31109 (4)	0.0063 (2)	1
Al2	32*g*	0.27779 (12)	0.19958 (12)	0.19068 (5)	0.0068 (2)	1
Al3	8*b*	0	$\frac{1}{4}$	$\frac{1}{8}$	0.0060 (3)	1

Table 3
Anisotropic atomic displacement parameters (Å^2) for $Al_9(Au;Ir)_4$.

Atom	U_{11}	U_{22}	U_{33}	U_{12}	U_{13}	U_{23}
Au1/Ir1	0.00365 (14)	0.00361 (13)	0.00224 (5)	0.00039 (3)	0	0
Au2/Ir2	0.00358 (4)	U_{11}	0.00390 (5)	0.00009 (3)	0	0
Al1	0.0084 (4)	0.0049 (4)	0.0057 (4)	0.0003 (3)	0.0004 (3)	0.0012 (3)
Al2	0.0049 (4)	0.0091 (4)	0.0064 (4)	0.0003 (3)	−0.0010 (3)	−0.0015 (3)
Al3	0.0080 (4)	U_{11}	0.0020 (6)	−0.0043 (5)	0	0

in agreement with the relatively intense unknown diffraction peaks found in the PXRD patterns. The presence of the AlIr compound could also be confirmed in another area of the sample. WDS has been carried out in several regions of the sample containing the new ternary phase in order to obtain a precise chemical composition. The measurements (200 points) lead to an average composition of $Al_{68.5(2)}Au_{2.4(2)}Ir_{29.1(2)}$.

3.2. Crystal structure analysis

A single crystal suitable for data collection was obtained by crushing the sample that provided the material for SEM analysis. Evaluation of the data set reveals a tetragonal unit cell with parameters a = 8.6339 and c = 21.8874 (7) Å. Because of the very similar scattering factors of Au and Ir, these atoms could not be differentiated when solving SC-XRD data and thus were considered only as Ir atoms. The crystal structure was successfully solved by direct methods in the tetragonal space group $I4_1/acd$ with 104 atoms in the unit cell. The reliability factors of this structure model are R_1(all) = 2.5% and wR_2(all) = 4.32%. From the chemical composition of $Al_{68.5}Au_{2.4}Ir_{29.1}$ given by WDS and considering the 104 atoms per unit cell given by the structure model, an average of 2.5 Au atoms is expected within the unit cell of this compound. This is consistent with a statistical distribution of the Au atoms on the Ir atomic positions, a feature expected for transition metals (TM) having a difference of only two electrons. A similar case of statistical distribution of Au/Ir atoms on the same atomic position was found in the Al_3AuIr crystal structure (Kadok *et al.*, 2015). Thus, the crystal structure of the new ternary phase has been refined considering that the TM sites were occupied with a mixed Au/Ir content. The occupancy ratio has been fixed to the value given by the WDS composition, *i.e.* considering 2.5 Au atoms among the 104 atoms of the unit cell which leads to a Au/Ir occupancy ratio of 0.08/0.92. Reliability factors did not significantly change after this refinement compared with the model considering only Al and Ir atoms. As given in the crystallographic data information in Table 1, the final chemical formula for this new compound is $Al_9Au_xIr_{4-x}$, $x = \frac{5}{16}$. Considering the mixed Au/Ir occupancy at certain atomic positions, the composition of this new compound is referred to as $Al_9(Au;Ir)_4$. However, during the exploration of the Al–Au–Ir system, this new compound could not be found with a gold content much higher than 2.5%, hence suggesting a narrow homogeneity range.

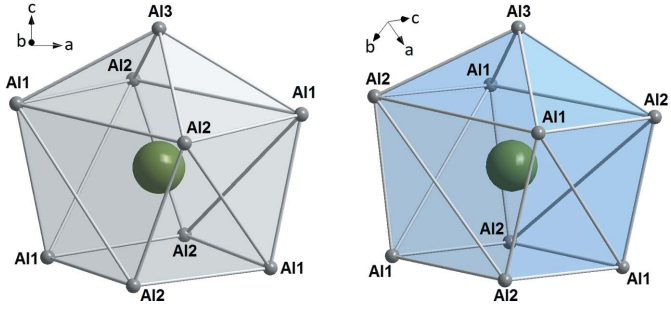

Figure 3
Coordination polyhedra around the Au1/Ir1 (left) and Au2/Ir2 (right) positions, having a twofold symmetry along the *c* and *a* axes, respectively.

The atomic positions and isotropic displacement parameters are listed in Table 2 and anisotropic displacement parameters in Table 3. In the structure of $Al_9(Au;Ir)_4$, the heavy atoms of Au and Ir are distributed in two 16-fold atomic positions. These two positions are each coordinated with a 9-Al polyhedron, both constituted of four Al1, four Al2 and one Al3 atoms. They can both be described by comparable capped quadratic prisms, one being slightly distorted compared with the other one. A representation of these atomic environments is depicted in Fig. 3 and a whole unit cell is shown in Fig. 4.

The isomorphic structure is found for the BGa_8Ir_4 compound (Kluenter & Jung, 1995). Compared with the $Al_9(Au;Ir)_4$ compound reported here, the Ir atoms in BGa_8Ir_4 are located at the 16*d* and 16*f* atomic positions (here Au1/Ir1 and Au2/Ir2, respectively), the Ga atoms at the two 32*g* positions (here Al1 and Al2) and the B atoms at the 8*b* positions (here Al3). As for the Ir—B bonds in BGa_8Ir_4, Au1/Ir1—Al3 and Au2/Ir2—Al3 are the shortest bonds in $Al_9(Au;Ir)_4$ (see Table 4). The similarity between these two crystal structures is not too surprising since B, Al and Ga belong to the same column of the periodic table. It is known that, within a given ternary system, substituting a TM or a metalloid element by an element of the same column of the periodic table can lead sometimes to an isomorphic structure (Tsai *et al.*, 1988).

The $Al_9(Au;Ir)_4$ compound reported here has a very low Au content, *i.e.* close to a binary Al–Ir compound. However, there are no similarities found with other crystal structures present in the Al–Ir system, although atomic positions of TM in $Al_9(Au;Ir)_4$ are shared by both Au and Ir, having a difference of two electrons. The requirement of partial substitution of Ir

Table 4
Main interatomic distances for Au1/Ir1 and Au2/Ir2 atoms in $Al_9(Au;Ir)_4$.

Atoms	Distance (Å)
Au1/Ir1—2Al1	2.5491 (10)
Au1/Ir1—2Al1	2.6589 (10)
Au1/Ir1—2Al2	2.5481 (10)
Au1/Ir1—2Al2	2.6262 (10)
Au1/Ir1—1Al3	2.41478 (15)
Au2/Ir2—2Al1	2.6113 (11)
Au2/Ir2—2Al1	2.6364 (10)
Au2/Ir2—2Al2	2.6086 (10)
Au2/Ir2—2Al2	2.6751 (11)
Au2/Ir2—1Al3	2.42465 (14)

by Au to stabilize this new structure may either have an electronic or an entropic origin. A Hume–Rothery-type stabilization mechanism is indeed frequently observed in Al–TM compounds in which a Fermi sphere–Brillouin zone interaction plays a key role to lower the total energy of the system. In this case, the Hume–Rothery condition $2k_F = K_{hkl}$ must be satisfied for some strong Bragg planes (Massalski & Mizutani, 1978; Trambly de Laissardière *et al.*, 2005). The Fermi vector can be estimated within a free electron model approximation and assuming an electron valence of +3 and +1 for Al and Au, respectively. A negative valence of −1.6 is attributed to Ir by Raynor (1949) while a more recent approach developed by Mizutani & Sato (2017) gives a value of +1.6. It leads to $2k_F = 2.88$ Å^{-1} or $2k_F = 3.35$ Å^{-1}, respectively. These values are close to K_{040} (2.91 Å^{-1}) and K_{228} (3.09 Å^{-1}) in the former case and close to K_{224} (3.45 Å^{-1}) in the latter case, all of these Bragg planes producing strong reflections. This suggests that the Hume–Rothery condition may be satisfied. However, the average number of valence electrons per atom is only weakly modified by the Au/Ir substitution (only 2.5 Au atoms per unit cell) and the Fermi wavevector is not significantly affected (it changes by only a few 10^{-2} Å^{-1}). Therefore the requirement for partial Ir/Au substitution is probably not of electronic origin but rather entropic.

A comparable situation is found in the Al–Si–Ir system. Ongoing work is revealing the existence of a new ternary compound where Si atoms are statistically distributed among the Al atomic positions (Kadok *et al.*, 2019). The latter also has a low content of Si, an element which has one electron more than Al. Further details concerning the stability of such a compound will be given in an upcoming report.

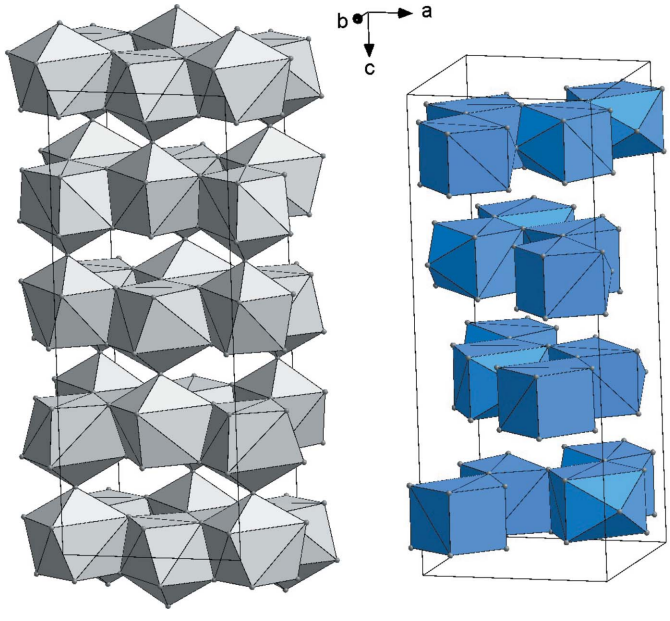

Figure 4
Distribution of the Al polyhedra built around the Au1/Ir1 (left) and Au2/Ir2 (right) atomic positions in the unit cell of the $Al_9(Au;Ir)_4$ compound reported here. Au1/Ir1 polyhedra are connected by sharing Al3 positions along the *c* axis and Al1–Al1 or Al2–Al2 edges in the (*ab*) plane. Au2/Ir2 polyhedra are only connected in the (*ab*) plane by sharing Al3 positions or Al1–Al2 edges.

4. Conclusion

$Al_9(Au;Ir)_4$ is the latest ternary compound reported for the Al–Au–Ir system. Just as for Al_3AuIr, the atomic structure shows a statistical distribution of the Au and Ir atoms on the same atomic positions. This phenomenon is likely to arise from the close chemistry between these two elements which differ by only two in the number of electrons they possess. With 104 atoms in a tetragonal crystal system, the $Al_9(Au;Ir)_4$ compound is isostructural to BGa_8Ir_4, with well-defined atomic clusters of Al surrounding TM atoms. The exploration of the Al-rich side of the Al–Au–Ir system will be pursued to unveil possible additional ternary compounds.

Acknowledgements

Christine Gendarme from the CC3M of the IJL is acknowledged for the WDS measurements.

Funding information

Funding for this research was provided by: Centre National de la Recherche Scientifique; Conseil Régional de Lorraine.

References

Bruker (2004). *APEX2*. Bruker AXS Inc., Madison, Wisconsin, USA.
Dubois, J.-M. & Belin-Ferré, E. (2011). Editors. *Complex Metallic Alloys: Fundamentals and Applications.* Weinheim, Germany: Wiley-VCH Verlag GmbH & Co.
Kadok, J. (2019). In preparation.
Kadok, J., de Weerd, M.-C., Boulet, P., Gaudry, E., Grin, Y., Fournée, V. & Ledieu, J. (2015). *Inorg. Chem.* **54**, 7898–7905.
Kluenter, W. & Jung, W. (1995). *Z. Anorg. Allg. Chem.* **621**, 197–200.
Krause, L., Herbst-Irmer, R., Sheldrick, G. M. & Stalke, D. (2015). *J. Appl. Cryst.* **48**, 3–10.
Massalski, T. & Mizutani, U. (1978). *Prog. Mater. Sci.* **22**, 151–262.
Mizutani, U. & Sato, H. (2017). *Crystals*, **7**, 9.
Okamoto, H. (1991). *J. Phase Equilib.* **12**, 114–115.
Okamoto, H. (2009). *J. Phase Equilib. Diffus.* **30**, 206–207.
Raynor, G. V. (1949). *Prog. Met. Phys.* **1**, 1–76.
Sheldrick, G. M. (2008). *Acta Cryst.* A**64**, 112–122.
Trambly de Laissardière, G., Nguyen-Manh, D. & Mayou, D. (2005). *Prog. Mater. Sci.* **50**, 679–788.
Tsai, A., Inoue, A. & Masumoto, T. (1988). *Jpn. J. Appl. Phys.* **27**, L1587–L1590.